Fluorescent Nanoparticles for Western Blotting

Kevin McDonald, Ahmed Elbaggari, and Marina Pekelis, Bio-Rad Laboratories, Inc., Hercules, CA 94547 USA

Introduction

Western blotting (Towbin et al. 1979, Renart et al. 1979) is a powerful method for identifying and analyzing protein targets. Many immunological detection systems have been developed to identify specific proteins blotted onto membranes, including autoradiographic, colorimetric, chemiluminescent, bioluminescent, chemifluorescent, fluorescent, and immunogold detection systems. These methods differ in their speed, sensitivity, and compatibility with multiplexing and quantitation.

Chemiluminescence is the predominant detection method for western blots, due to its speed and sensitivity compared to other methods (Kurien and Scofield 2003). Detection of protein in low picogram amounts is typical for chemiluminescent systems; these are more sensitive than most colorimetric systems, and approximately equal in sensitivity to radioisotopic detection. The biggest disadvantage of chemiluminescent detection is its incompatibility with multiplexing.

Another common method for identifying blotted proteins is fluorescence detection. Fluorescence detection can provide a 10-fold greater linear dynamic range than chemiluminescent methods, therefore providing better quantitation within the detection limits. Fluorescence detection also allows multiplex experiments to detect multiple antigens in a single probing step. Unfortunately, the sensitivity of most fluorescent blotting techniques is 2–4 times lower than that of analogous luminescence methods (Bio-Rad bulletin 2895).

Use of fluorescent semiconductor nanocrystals, or quantum dots (QDs), can overcome many of the handicaps of fluorescence detection, because QDs have unique optical properties that make them highly sensitive and well suited for optical multiplexing. First, unlike organic fluorophores, which absorb light of a particular wavelength, QDs absorb all wavelengths of light shorter than their emission wavelength. Therefore, a single light source emitting blue or shorter wavelengths can excite all QDs in a multiplex experiment, thereby significantly decreasing the cost and complexity of the setup. Second, the emission spectra of QDs, averaging 30 nm wide, are much more symmetrical than those of organic fluorophores. This affects both sensitivity and the ability to detect multiple targets in one imaging session. Because the emission spectra of organic fluorophores typically have extra peaks and long red tails, there can be considerable cross talk between channels. This cross talk decreases signal-to-noise ratio, and thus sensitivity. In contrast, the overlap between spectra of QDs is significantly less than for organic fluorophores (Alivisatos 1996). Furthermore, since the emission from QDs is concentrated in a narrow band, detection can be accomplished with narrow bandpass filters, which reject more background noise and autofluorescent contamination, increasing the sensitivity of detection. Finally, QDs are more photostable than organic fluorophores. This means that QD-labeled samples can be irradiated for long periods to improve sensitivity for better quantitation and reliability (Chan and Nie 1998, Wu et al. 2003).

In this article, we demonstrate the sensitivity and multiplex application of commercially available QD conjugates (Qdot conjugates from Invitrogen Corp.; originally developed by Quantum Dot Corp.) with various excitation and detection techniques, taking advantage of the flexibility of emission filter configuration allowed by Molecular Imager® VersaDoc™ and PharosFX™ systems. We also compare the detection limits of Qdot fluorescence and horseradish peroxidase (HRP) conjugate-based chemiluminescence.

Methods

Detection of Qdot QDs With Filters

Broad range biotinylated molecular weight standards (Bio-Rad catalog #161-0319) were separated on a Criterion™ 8–16% linear gradient gel, then transferred to an Immobilon-FL transfer membrane (Millipore Corp.). The blot was blocked with TBST buffer (Tris-buffered saline (TBS, 170-6435) containing 0.05% Tween 20 (161-0781)) and 3% dry milk (170-6404), then cut into vertical strips for detection with seven different streptavidin Qdot conjugates (Invitrogen #Q10151MP). Qdot QDs were diluted 1:1,000 in blocking solution. Fluorescence was detected on a PharosFX imager with 488 nm laser excitation and a VersaDoc 4000 imager with epi-UV excitation. The strips were imaged twice using different filters: those included with the instruments, and the Qdot-specific filters from Omega Optical Inc., recommended by Invitrogen.

On the PharosFX imager, Qdot-specific filters were inserted into blank filter cubes and added to the acquisition software according to the PharosFX instructions. The Qdot-specific filter was inserted in place of the clear glass in position 4 of the VersaDoc filter wheel and secured with a 25 mm diameter friction ring inserted on top of the filter. The 660SP filter was removed from the lens. In Quantity One® image acquisition software, a custom application was defined using filter position 4 for imaging the sample.

Comparison of Qdot Fluorescence and HRP-Based Chemiluminescence

To compare the detection limits of Q655 Qdot (Invitrogen) and Immun-Star™ HRP substrate, human transferrin (Sigma-Aldrich, Sweden) was detected using the dot-blot method. A series of 2-fold transferrin dilutions, beginning at 200 ng/ml, were made in 100 µg/ml bovine serum albumin (BSA) in TBS. A BSA solution was used as a control. A 50 µl aliquot of each dilution was loaded onto a Bio-Dot® microfiltration unit. The apparatus and protein solutions were left at room temperature (RT) for 2 hr before the solutions were drawn through the nitrocellulose membrane (162-0145) by applying a vacuum to the apparatus for about 10 min. The wells were washed twice with 200 µl TBS, which was drawn through the membrane in the same manner. The membrane was removed from the apparatus, cut in half, and blocked with Qdot blocker solution (Invitrogen) overnight at 4°C. After blocking, the membrane was incubated at RT for 1 hr with 1:6,000 rabbit anti-human transferrin antibody (Dako A/S, Denmark) in Qdot blocker. After 5 x 5 min washes in TBST, the two membrane pieces were placed in separate trays and incubated for 1 hr at RT with either 1:1,000 Qdot 655-conjugated goat anti-rabbit antibody (Invitrogen #Q11421MP) in Qdot blocker or with 1:15,000 HRP-conjugated goat anti-rabbit antibody (170-5046). The membranes were washed as before, then the Qdot 655 blot was placed in TBS while the HRP blot was incubated for 5 min in 12 ml Immun-Star HRP substrate. The HRP blot was then placed in a sheet protector to prevent drying out during imaging. The chemiluminescent HRP blot was imaged first to capture maximum signal intensity.

Blots were imaged with a VersaDoc 4000 using 4 x 4 binning for acquisition. Integration time was 3.5 sec for the Qdot blot and 4 min for the chemiluminescent blot. A 50 mm lens and 655bp20 filter (Omega Optical) were used to image the Qdot 655 blot.

Western Blotting With Qdot Conjugates

C166-GFP mouse endothelial cells stably expressing the Green Fluorescent Protein (GFP) gene (obtained from ATCC #CRL-2583) were transfected with siLentFect™ lipid reagent and 5 nM of several siRNA-GFP duplexes that had different predicted knockdown efficiencies: negative control (scramble), siRNA-X, siRNA-Y, and siRNA-Z. Cells were lysed 24 hr posttransfection in Laemmli sample buffer containing 5% β-mercaptoethanol in a total volume of 125 µl and incubated at 85°C for 5 min. Protein was quantitated using an Experion™ Pro260 analysis kit, after which 10–40 µg was separated on Ready Gel® 4–15% Tris-HCl gels and then transferred in Towbin buffer to Immobilon-FL membranes using the Mini Trans-Blot® cell following manufacturer instructions. After transfer, the membrane was incubated in blocking buffer for 1 hr at RT with agitation. The membrane was then incubated for 1 hr in blocking buffer containing 1:400 mouse anti-glyceraldehyde-3-phosphate dehydrogenase (GAPDH) (Ambion, Inc.) and rabbit anti-GFP (BD Biosciences). After three washes with TBST, the blot was incubated for 1 hr in blocking buffer containing 1:1,000 Qdot 605-goat anti-mouse, Qdot 655-goat anti-rabbit, and Qdot 705-streptavidin conjugates. The blot was washed three times in TBST, then three times in TBS. Finally, the blot was imaged with a VersaDoc 4000 imager and emission filters specific to Qdot 605, 655, and 705 (Omega Optical).

Results and Discussion

Optimizing Excitation of QDs

Two factors to consider when selecting an excitation source for QDs are wavelength and power output. Although any light source that emits wavelengths shorter than the emission spectrum of the QD can be used, the extinction coefficient of QDs (and thus the probability that light will be absorbed) is greater at shorter wavelengths (Quantum Dot 2005). Therefore, short wavelengths are generally more efficient and will result in a brighter signal. On the other hand, light sources of greater wavelength can have a higher power output, and in some cases this compensates for the lower extinction coefficient.

The standard excitation source for Molecular Imager FX™ and PharosFX laser scanners is a 532 nm laser, which can excite all QDs with an emission of greater wavelength. An external 488 nm laser is also available. For the PharosFX imager, however, the power output of the 532 nm laser is typically 2-fold greater than that of the 488 nm laser, and this translates to approximately twice the photon density. This large difference in photon density compensates for the lower extinction coefficient, and therefore the standard 532 nm laser is generally satisfactory for all QDs other than those with emission below 532 nm, which must be excited with the 488 nm laser.

The most common excitation source included with CCD imagers, including VersaDoc, ChemiDoc™, and Gel Doc™ imagers, is a broad range UVB lamp, which has a peak wavelength output of 302 nm. This source is suitable for all Qdot QDs we tested. Although UV lamps deliver a low photon density compared to lasers, the VersaDoc imager is still a practical imager for QDs, since 302 nm light is highly efficient in exciting QDs.

Selection of Emission Filters for Detection of Qdot QDs With PharosFX and VersaDoc 4000 Imagers

The performance of QDs in multiplex fluorescence detection largely depends on selection of tools for fluorescence excitation and detection. Standard emission filters of PharosFX (Table 1) and VersaDoc 4000 (Table 2) imagers are suitable for detecting some Qdot QDs. But because these filters are not optimally aligned to the emission peaks of the Qdot QDs, they do not allow the highest possible sensitivity and spectral separation.

The brightest Qdot QDs detected by the PharosFX imager were the 655, 705, and 800 dots; dots with shorter wavelength emission were far dimmer (Figure 1A). Thus, the standard filters are of limited use for 565, 585, and 605 dots. Nonetheless, when the 488 nm laser is used, the PharosFX imager can efficiently distinguish pairs of dots for multiplex applications. Acceptable dot combinations for multiplex detection with standard filters are listed in Table 1. Although visual separation of dot pairs is possible, the low intensity of the Qdot QDs that emit below 655 nm would require the sample being detected to be at relatively high abundance.

As expected, narrow bandpass filters aligned to the emission peaks of the Qdot QDs produced higher sensitivity and better spectral separation. The number of dot combinations acceptable for multiplexing is greater when Qdot-specific filters are used (Table 3). Furthermore, with Qdot-specific filters, all dots were detected when the 488 nm laser was used (Figure 1B). Similar results would be expected when using the 532 nm laser, except 525 dots cannot be used.

The VersaDoc 4000 imager excited the shorter wavelength dots more efficiently than the PharosFX imager (Figure 2A). This was expected because of the greater extinction coefficient in the UV spectra by QDs. Due to the transmission ranges of the standard filters, however, only the three dot combinations shown in Table 2 can be dependably distinguished.

As with the PharosFX imager, use of Qdot-specific filters on the VersaDoc imager allows a broader range of dot combinations to be used (Table 4). The intensity of emission of Qdot 525, 565, 585, and 605 upon UV excitation makes them more practical as multiplex partners than they are with visible light excitation (Figure 2B).

Comparison of Sensitivity of Qdot QDs and HRP-Chemiluminescent Labeling of Dot Blots

The sensitivity of protein detection with Qdot conjugates was similar to that with Immun-Star HRP substrate, when normalized to a BSA control (Figure 3A, B), but Qdot QDs displayed better linearity at lower concentrations of protein (Figure 3C). The HRP blot, however, had a lower membrane background signal in the area between wells — more than an order of magnitude lower than that of the closest Qdot 655 data. Use of low-fluorescence membrane would provide an improvement in the signal-to-background ratio for Qdot blots.

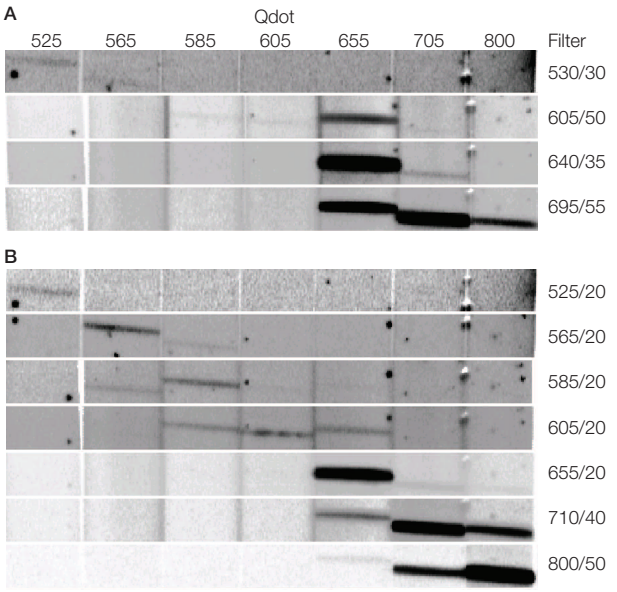

Fig. 1. Detection of Qdot QDs on the PharosFX imager. Qdot QDs with different emission peaks were detected using standard (**A**) or Qdot-specific (**B**) filters.

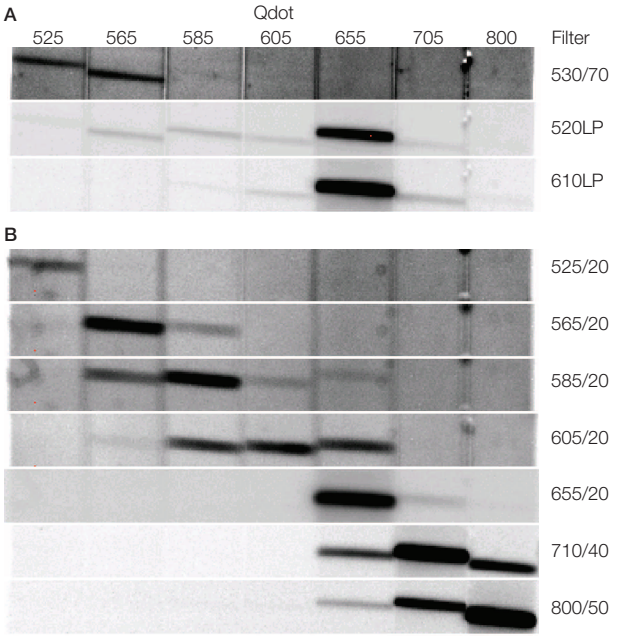

Fig. 2. Detection of Qdot QDs on the VersaDoc 4000 imager. Qdot QDs with different emission peaks were detected using standard (**A**) or Qdot-specific (**B**) filters.

Table 1. Acceptable Qdot combinations for 488 laser excitation and standard PharosFX filters.

Dot 1	Filter 1	Dot 2	Filter 2
525	530/30	655	640/35
525	530/30	705	695/55
525	530/30	800	695/55

Table 2. Acceptable Qdot combinations for UV excitation and standard VersaDoc 4000 filters.

Dot 1	Filter 1	Dot 2	Filter 2
525 or 565	530/70	655	610LP
525 or 565	530/70	705*	610LP
525 or 565	530/70	800*	610LP

* With 660SP filter removed from lens.

Table 3. Acceptable Qdot combinations for 488 nm laser excitation and Qdot-specific filters.

	525	565	585	605	655	705	800
525	—	•	•	•	•	•	•
565	•	—	∘	•	•	•	•
585	•	∘	—	∘	•	•	•
605	•	•	∘	—	∘	•	•
655	•	•	•	∘	—	∘	•
705	•	•	•	•	∘	—	∘
800	•	•	•	•	•	∘	—

• = Optimal combination of Qdot QDs for multiplexing.
∘ = Suboptimal combination of Qdot QDs; some spectral overlap can be observed.

Table 4. Acceptable Qdot combinations for UV excitation and Qdot-specific filters.

	525	565	585	605	655	705	800
525	—	•	•	•	•	•	•
565	•	—	∘	•	•	•	•
585	•	∘	—	∘	•	•	•
605	•	•	∘	—	∘	•	•
655	•	•	•	∘	—	∘	∘
705	•	•	•	•	∘	—	∘
800	•	•	•	•	∘	∘	—

• = Optimal combination of Qdot QDs for multiplexing.
∘ = Suboptimal combination of Qdot QDs; some spectral overlap can be observed.

Multiplex Western Blotting With an Internal Standard for Better Quantitation

Multiplex western blotting can be used to verify that an equal quantity of protein is being loaded onto each lane of the gel, e.g., by probing a housekeeping protein along with the antigen of interest in each sample. This is important for quantitative applications. Such an experiment is shown in Figure 4. Expression levels of GFP in a stably transfected cell line were altered using siRNA from the GFP gene. GAPDH was chosen as an internal standard. Probing the blot with antibodies for both antigens allowed normalization of GFP expression. As shown in Figure 4, expression levels of GFP were quite different when comparing direct GFP volume values to those normalized to the GAPDH volume values.

According to the uncorrected data, the treatment with siRNA-Z produced the least efficient silencing (highest value of GFP concentration on the blot) of the GFP gene. However, the normalized data shows that the treatment with siRNA-Z ranked third of the four treatments in the extent of downregulation of the GFP expression, with least efficient silencing observed in the control treatment.

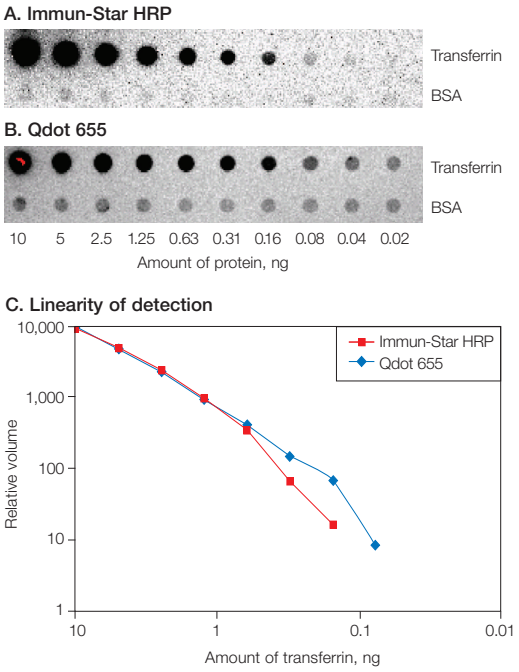

Fig. 3. Comparison of chemiluminescence and Qdot fluorescence. Dot blots were labeled with Immun-Star HRP (**A**) or Qdot 655 (**B**) and imaged with a VersaDoc 4000 imager. Integration time was 4 min for Immun-Star HRP and 3.5 sec for Qdot 655. **C**, plot of relative dot volume vs. amount of loaded protein. R^2 values were 0.9968 for Immun-Star HRP, 0.9992 for Qdot 655.

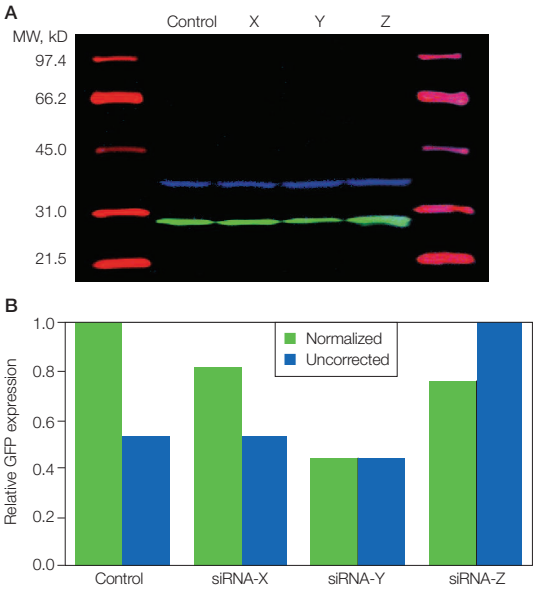

Fig. 4. Multiplex western blot detection of GAPDH and GFP expression in C166-GFP endothelial cells. Cells were transfected with four different siRNA-GFPs (X, Y, Z, or a scrambled control). **A**, visualization using the Qdot-conjugated antibodies to GFP (green), GAPDH (blue), and biotinylated protein standards (red) described in Methods. The image was acquired with a VersaDoc 4000 imager using QD-specific emission filters. **B**, GFP expression relative to GAPDH. GFP expression levels from the blot were corrected for variations in protein loading and transfer using a correction factor F, where $F = [GAPDH_{control}]/[GAPDH_x]$, and x refers to lanes X, Y, or Z of the blot. Normalized GFP expression is then [GFP]/F.

Conclusions

Fluorescent nanoparticles such as Qdot QDs can serve as excellent visualization labels for multiplex western blotting. Qdot QDs provided higher data quality than chemiluminescent blotting, due to better linearity at low concentrations of antigen, and the capability of using internal standards on the same blot.

The versatile functionality and optimized fluorescence detection of the VersaDoc 4000 and PharosFX systems can be used to image QD-labeled, multiplex western blots with detection sensitivity equivalent to that of chemiluminescence detection.

Acknowledgements

We thank Marcel Bruchez (Invitrogen Corporation) for Qdot materials and technical consultations, and Teresa Rubio (Bio-Rad) for applications related to RNAi methods and samples for western blotting.

References

Alivisatos AP, Semiconductor clusters, nanocrystals, and quantum dots, Science 271, 933–937 (1996)

Bio-Rad Laboratories, Inc., Protein blotting guide, Bio-Rad bulletin 2895

Chan WC and Nie SM, Quantum dot bioconjugates for ultrasensitive nonisotopic detection, Science 281, 2016–2018 (1998)

Kurien BT and Scofield RH, Protein blotting: a review, J Immunol Methods 274, 1–15 (2003)

Quantum Dot Corporation, Qdot nanocrystals, http://www.qdots.com/live/render/content.asp?id=84 (2005)

Renart J et al., Transfer of proteins from gels to diazobenzyl-oxymethyl-paper and detection with antisera: a method for studying antibody specificity and antigen structure, Proc Natl Acad Sci USA 76, 3116–3120 (1979)

Towbin H et al., Electrophoretic transfer of proteins from polyacrylamide gels to nitrocellulose sheets: procedure and some applications, Proc Natl Acad Sci USA 76, 4350–4354 (1979)

Wu X et al., Immunofluorescent labeling of cancer marker Her2 and other cellular targets with semiconductor quantum dots, Nat Biotechnol 21, 41–46 (2003)

Information in this tech note was current as of the date of writing (2005) and not necessarily the date this version (rev A, 2006) was published.

Bio-Rad
Laboratories, Inc.

Life Science
Group

Web site www.bio-rad.com **USA** 800 4BIORAD **Australia** 02 9914 2800 **Austria** 01 877 89 01 **Belgium** 09 385 55 11 **Brazil** 55 21 3237 9400
Canada 905 712 2771 **China** 86 21 6426 0808 **Czech Republic** 420 241 430 532 **Denmark** 44 52 10 00 **Finland** 09 804 22 00 **France** 01 47 95 69 65
Germany 089 318 84 0 **Greece** 30 210 777 4396 **Hong Kong** 852 2789 3300 **Hungary** 36 1 455 8800 **India** 91 124 4029300/5013478 **Israel** 03 963 6050
Italy 39 02 216091 **Japan** 03 5811 6270 **Korea** 82 2 3473 4460 **Mexico** 55 5200 05 20 **The Netherlands** 0318 540666 **New Zealand** 64 9415 2280
Norway 23 38 41 30 **Poland** 48 22 331 99 99 **Portugal** 351 21 472 7700 **Russia** 7 095 721 14 04 **Singapore** 65 6415 3188 **South Africa** 27 0861 246 723
Spain 34 91 590 5200 **Sweden** 08 555 12700 **Switzerland** 061 717 95 55 **Taiwan** 886 2 2578 7189/2578 7241 **United Kingdom** 020 8328 2000

Bulletin 3179 US/EG Rev A 05-0626 0706 Sig 1205